HOSTED BY

ELSEVIER

CrossMark

Available online at www.sciencedirect.com

ScienceDirect

Progress in Natural Science: Materials International 26 (2016) 24–31

Progress in Natural Science Materials International

www.elsevier.com/locate/pnsmi
www.sciencedirect.com

Original Research

Growth and properties of semi-organic nonlinear optical crystal: L-Glutamic acid hydrochloride

J. Uma*, V. Rajendran

Department of Physics, Presidency College, Chennai, India

Received 29 January 2015; accepted 25 June 2015
Available online 10 February 2016

Abstract

Semiorganic nonlinear optical crystal of L-Glutamic acid hydrochloride (LGHC) was grown from aqueous solution by slow evaporation technique. Single crystal X-ray Diffraction analysis confirms that LGHC crystallizes in orthorhombic system with noncentrosymmetric space group $P2_12_12_1$. The powder X-ray diffraction study confirms the crystallinity of the grown crystal. The fundamental functional groups of the grown crystals were analyzed by Fourier Transform Infrared spectroscopic analysis in the range of 450–4000 cm^{-1}. The range of optical transmission was ascertained using UV–vis–NIR studies. The Refractive Index of the LGHC crystal was found to be 1.4. The second harmonic generation efficiency of the LGHC was determined using Kurtz and Perry powder technique and it was 0.5 times greater than that of the KDP crystal. Thermo Gravimetric Analysis (TGA) and Differential Thermal Analysis (DTA) were used to study thermal behavior of the sample. The dielectric behavior and ac conductivity of the sample were studied as a function of frequency for different temperatures. The mechanical strength of the crystal was determined by Vicker's Hardness test. The elastic stiffness constant and yield strength of the sample was calculated.

Keywords: Semi organic nonlinear optical crystal; X-Ray Diffraction; UV–vis–NIR; Dielectric study; Microhardness

1. Introduction

The design of devices that utilize photons instead of electrons in the transmission of information has created a need for new materials with unique optical properties [1]. Extensive efforts were made in recent years to develop new inorganic, organic and semi organic nonlinear optical (NLO) materials that possess properties such as high threshold, wide transparency range and high nonlinear coefficient which make them suitable for frequency doubling [2]. Semiorganic materials are attracting a great deal of attention in the field of nonlinear optics [3]. In semiorganic materials, the organic ligand is ionically bonded with inorganic host that resulted in new materials having high optical nonlinearities [4]. Complexes of amino acids with inorganic salts are promising materials for optical applications such as optical communication, optical computing, optical information processing, optical disk data storage, laser fusion reaction, laser remote sensing.

L-Glutamic acid is a phase matchable NLO material that has high transparency in the UV region [5]. L-Glutamic Acid has an acidic carboxyl group on its side chain, which serves as both an acceptor, and a donor of ammonia, and is the main NLO active chromophore [6]. Earlier study reported includes the growth and characterization of L-glutamic acid crystals with halogen compounds were L-glutamic HCl [7,8], L-glutamic acid and halogen salts [9]. Sathyalakshmi et al reported the growth and characterization of pure and doped L-glutamic acid hydrochloride [6]. Selvaraju et al reported metastable zone width, induction period for L-glutamic hydrochloride crystal that was grown by low temperature solution growth method [10] and its growth and characterization by slow evaporation method [11]. Bairava Ganesh et al reported Sankaranarayanan-Ramasamy (SR) method of uniaxial growth of L-glutamic hydrochloride crystal and its comparative studies [12].

*Corresponding author. Research Scholar, Presidency College. Tel.: +91 44 26561236.
E-mail address: kanarayanaphd70@gmail.com (J. Uma).
Peer review under responsibility of Chinese Materials Research Society.

http://dx.doi.org/10.1016/j.pnsc.2016.01.013

The present investigation deals with the growth and characterization of L-Glutamic acid hydrochloride (LGHC) single crystal by slow evaporation solution growth technique. The grown crystal was subjected to single crystal X-Ray Diffraction, powder X-Ray Diffraction, FT-IR, UV–vis–NIR, refractive index, SHG, TG/DTA, dielectric and mechanical studies.

2. Experimental procedure

2.1. Synthesis

L-Glutamic acid Hydrochloride (LGHC) was synthesized by slow evaporation solution growth technique from aqueous solution containing L-Glutamic acid (Extra pure grade, Merck) and Hydrochloric acid (GR grade) of 99% purity in 1:1 stoichiometric ratio. The resultant solution was filtered and allowed to evaporate at room temperature. Optically good quality crystals were harvested over a period of 20 days. The purity of the synthesized material was improved by the repeated recrystallization. The most essential feature of growth of high optical quality crystal is the purification of the material. It is essential to increase the purity to reputable level before proceeding further to get the better quality crystal [13]. The as grown crystals of LGHC are shown in Fig. 1. The LGHC was synthesized on the following reaction

$$HOOC(CH_2)_2CH(NH_2)COOH + HCl \rightarrow HOOC(CH_2)_2CH(NH_3)COOH \cdot Cl$$

2.2. Solubility

The solubility of synthesized LGHC crystal was determined by dissolving the crystals in deionized water taken in an air tight container, maintained at a constant temperature with continuous stirring. After attaining the saturation, the equilibrium concentration of the solute is analyzed gravimetrically. The temperature dependence of solubility of the LGHC is shown in Fig. 2. From the graph, it is found that the solubility of the LGHC increases with temperature and possesses positive gradient of solubility.

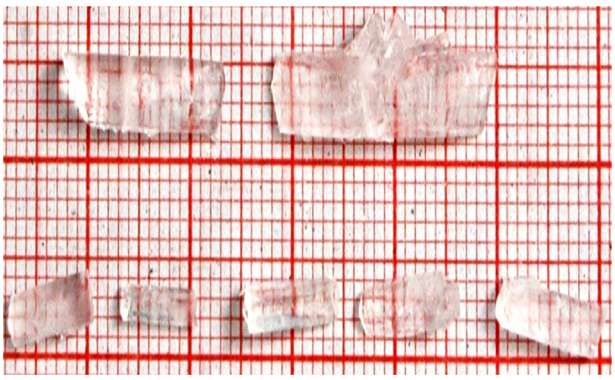

Fig. 1. As grown crystal of LGHC.

3. Results and discussion

3.1. Single crystal and powder X-ray diffraction analysis

Single crystal X-ray diffraction data were recorded using Bruker Kappa APEXII X-ray diffractometer with MoKα radiation ($\alpha = 0.7107$ Å) at room temperature. The LGHC crystal belongs to orthorhombic system with the space group of $P2_12_12_1$. The cell parameters of the grown crystals are $a = 5.1317$ Å (± 0.01), $b = 11.7290$ Å(± 0.001), $c = 13.2767$ Å(± 0.02), and $V = 799.1134$ Å^3(± 0.01) and are in good agreement with the earlier reported values [7,14]. The single crystal XRD results are tabulated in Table 1.

Powder X-ray diffraction pattern was recorded using CuKα (K = 1.5418 Å) radiation by crushing the LGHC crystal into fine powder. The diffraction pattern is shown in Fig. 3 that confirms the perfection of good quality single crystal. The appearance of quiet sharp diffraction peaks shows that the LGHC crystal is free from structural grain boundaries and the crystalline nature is good [15].

3.2. FT-IR spectral analysis

The FT-IR spectra of the grown crystal were recorded in the KBr phase in the frequency range of 450–4000 cm^{-1} using a

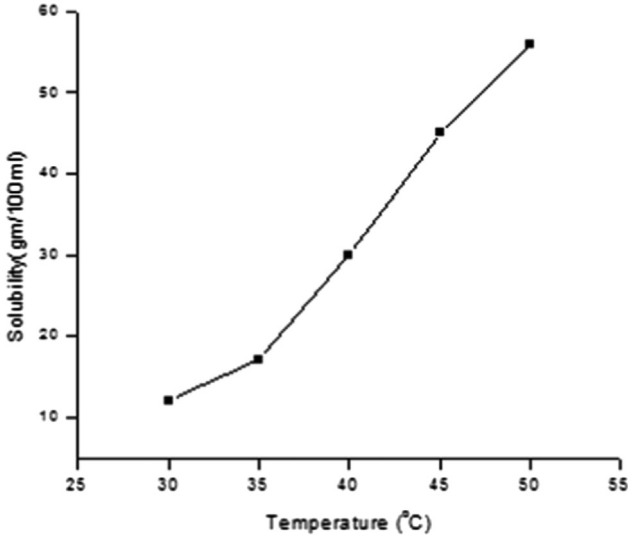

Fig. 2. Solubility curve of LGHC.

Table 1
Single Crystal XRD results.

Chemical formula	$HOOC(CH_2)_2CH(NH_3)COOH \cdot Cl$
Crystal System	orthorhombic
Space group	$P2_12_12_1$
a (Å)	5.1317
b (Å)	11.7290
c (Å)	13.2767
$\alpha = \beta = \gamma$ (deg)	90
Volume (Å^3)	799.1134

Perkin Elmer Spectrum1 FT-IR spectrometer as shown in Fig. 4. The broad peak observed between 3400–2500 cm^{-1} is assigned to O–H stretching vibration which overlaps with the peaks corresponding to N–H stretching vibration due to the primary amines (–NH_2) at 3000 cm^{-1} and C–H stretching vibration modes around 2900 cm^{-1} [16]. The peak at 1682 cm^{-1} is due to C=O stretching. It is slightly shifted due to the compound formation. The compound formation occurs in such a way that the primary amide group –NH_2 is combined with the HCl and gives $NH_3^+Cl^-$ by forming the bond between the chlorine atom of HCl with the amide group of L-glutamic acid [14]. Chlorine anions act as acceptors and connect two adjacent carboxylic groups of L-glutamic acid through the hydrogen bonding interaction. This interaction enhances the NLO activity of the LGHC crystal and makes it suitable for optoelectronic application. The peak observed at 1608 cm^{-1} corresponds to NH_3^+ vibration. C–H and O–H bending vibration modes show absorption peaks at 1425 and 999 cm^{-1} respectively. The C–O stretching vibration shows an absorption peak at 1210 cm^{-1}. The functional group assignments of LGHC crystal are given in Table 2.

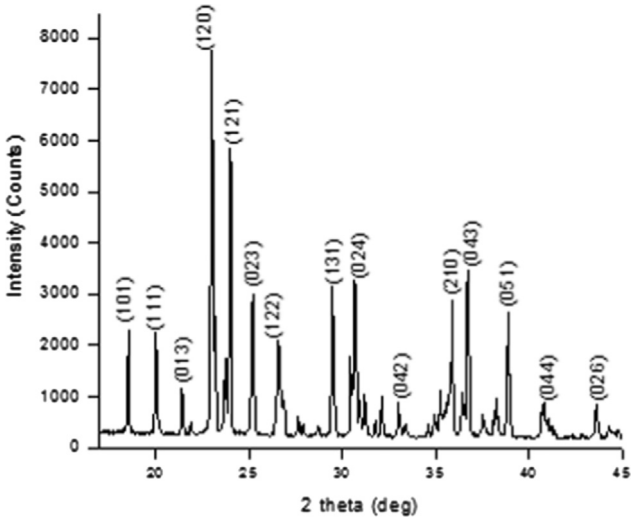

Fig. 3. Powder X-Ray Diffraction of LGHC.

3.3. UV–vis–NIR spectral analysis

The UV–vis–NIR absorption spectrum of the LGHC crystal was recorded in the range of 200–2000 nm using a Cary Varrian UV-vis-NIR spectrophotometer and is shown in Fig. 5. It is observed that there is low absorbance in the entire visible and IR regions. It is evident that LGHC has a very low UV cutoff wavelength at 248 nm which is sufficient for Second Harmonic Generation. At lower temperatures the active trapping of impurities by the growing crystals leads to the formation of different defects that result to the increase of optical absorption or decrease of transmission [17]. The decrease in the percentage of optical absorption in LGHC crystal may be due to the absent of solvent inclusion which in turn reduces the scattering centers and increase the output intensity [18]. The transparency nature in the entire visible and IR region is the desired criteria for NLO applications.

Table 2
FTIR functional group assignments of LGHC crystal.

Wavenumbers (cm^{-1})	Assignments
489	NH_3^+ torsion
534	COO^- wagging
633	NH_3 deformation
674	COO^- in-plane deformation
792	O–H in-plane deformation
862	C–C stretching
999	O–H bending
1079	NH_3^+ rocking
1210	C–O stretching
1274	CH_2 twisting
1372	C–C–H in-plane deformation
1425	C–H bending
1508	NH_3^+ symmetric deformation
1608	NH_3^+ vibration
1682	C=O stretching
1722	COO^- stretching
2123	NH_3^+ degenerative deformation
2293, 2900,1980	C–H stretching
2623, 3000	N–H stretching

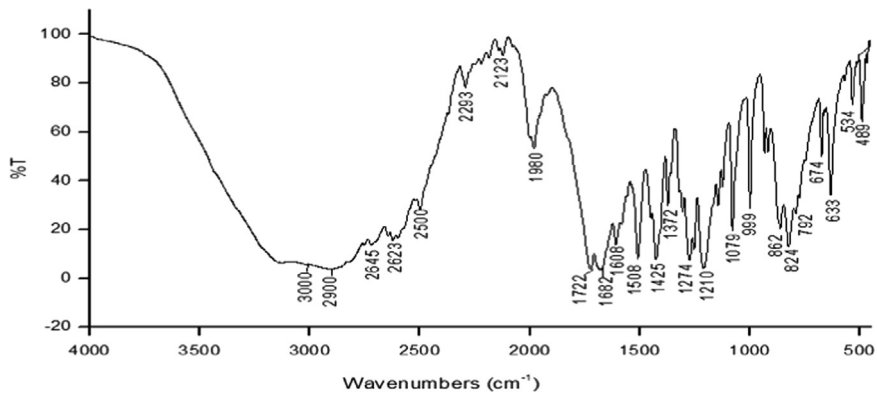

Fig. 4. FTIR spectrum of the grown LGHC crystal.

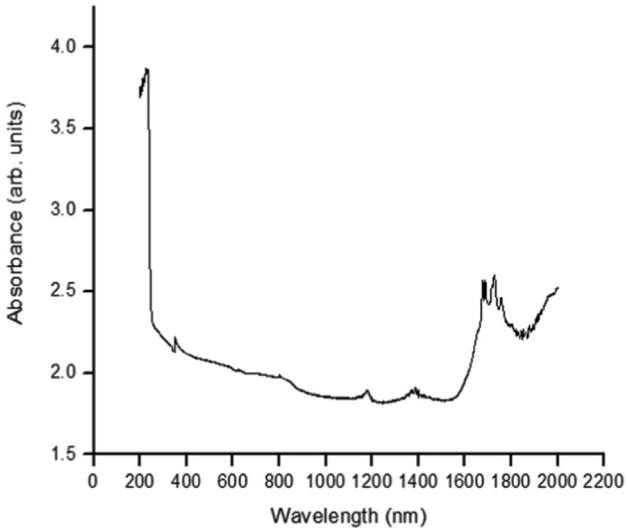

Fig. 5. UV Absorption spectrum of LGHC.

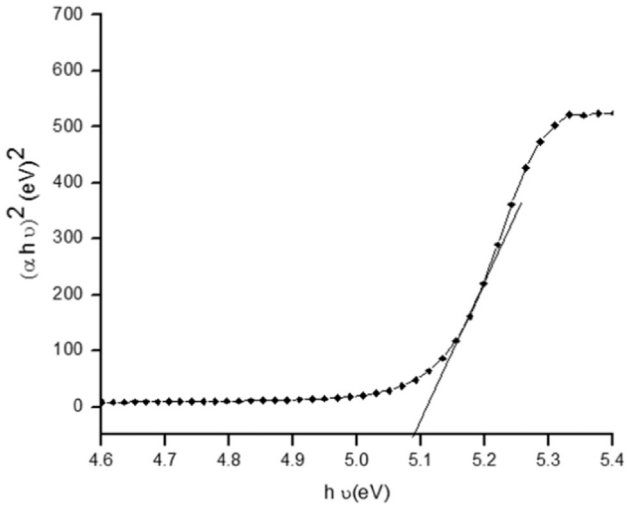

Fig. 6. Plot of $(\alpha h\nu)^2$versus $h\nu$ of LGHC.

The optical absorption coefficient (α) was calculated using Eq. (1)

$$\alpha = \left(\frac{2.303}{t}\right)\log\left(\frac{1}{T}\right) \quad (1)$$

where T is the transmittance and t is the thickness of the crystal. Optical band gap (E_g^{opt}) was evaluated from the absorption spectra and optical absorption coefficient (α) near the absorption edge [19] is given by Eq. (2).

$$(h\upsilon\alpha) = A\left(h\upsilon - E_g^{opt}\right)^{\frac{1}{2}} \quad (2)$$

where A is a constant, E_g^{opt} the optical band gap, h the Planck constant and υ the frequency of the incident photons. By plotting a graph between $(\alpha h\upsilon)^2$ versus hυ and extrapolating the linear portion near the onset of absorption edge to the energy axis [20], the band gap of LGHC crystal was estimated. From Fig. 6, the value of band gap was found to be 5.08 eV.

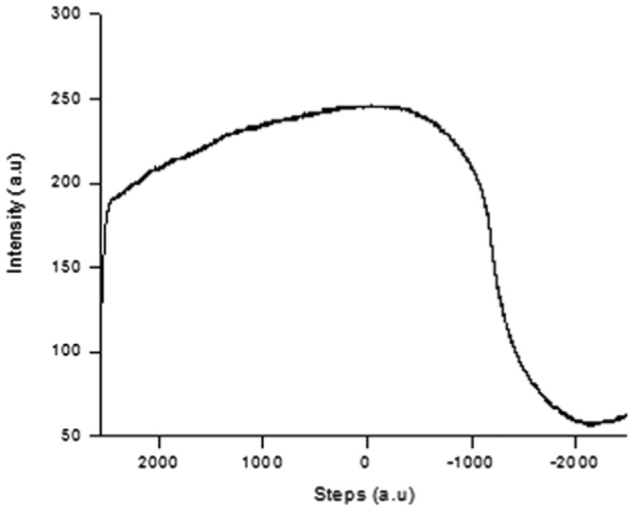

Fig. 7. Refractive index of LGHC.

3.4. Refractive index measurements

Refractive index of the LGHC was measured using Metricon model 2010 prism coupler. The resolution of the instrument was of ± 0.0005. A laser beam strikes the base of the prism and it is reflected normally at the prism base onto a photo detector. The Sample was brought into contact with the prism base by means of a coupling head. Nitrogen gas pressure was used to make a contact between the crystal and the prism. The angle of incidence 'θ' of the laser beam could be varied by means of a rotary table. The refractive index was determined by measuring the critical angle or mode angle "θ" for the sample-prism interface. The LGHC crystal shows a clear critical angle knee, from which the refractive index was calculated by an appropriate computer algorithm. The knee observed is shown in Fig. 7 and the calculated refractive index is 1.4.

3.5. Second harmonic generation

The second harmonic generation conversion efficiency of the LGHC was measured by the Kurtz and Perry powder technique [21]. The grown single crystal of the LGHC was powdered with a uniform particle size and then packed in a micro capillary of uniform bore and exposed to laser radiations. The fundamental beam of high-intensity ($\lambda = 1064$ nm) from Q- switched Nd:YAG laser with pulse duration of 8 ns with 10 Hz pulse rate was made to fall normally on the powdered sample cell. The second harmonic generation behavior was confirmed from the emission of green light ($\lambda = 532$ nm) and collected after separating the 1064 nm pump beam with an IR-blocking filter. SHG efficiency of the LGHC crystal is found to be 0.5 times greater than that of the KDP crystal. SHG efficiency of semiorganic crystals reported earlier is compared in Table 3.

3.6. Thermal analysis

The Thermo Gravimetric Analysis (TGA) and Differential Thermal analysis (DTA) were carried out for the LGHC crystal using TGA Q500 V20.10 Build 36 thermal analyzer in the temperature range of 50–850 °C in nitrogen atmosphere at a heating rate of 20 °C min^{-1}. The TGA and DTA graph is shown in Fig. 8. The studies reveal that LGHC is thermally stable up to 185 °C, after that the sample undergoes appreciable weight loss. The weight loss in the initial stage was 36.84% with a peak at 225 °C. The change in weight loss is due to the liberation of water molecules in the crystal, which confirms the decomposition nature of the sample. Above 270 °C, the weight loss was 49.09% and is due to the complex degradation of volatile compounds such as N, Cl and CO_2.The final stage of weight loss is 6.54% where the sample completely decomposes without any residue. From the studies it is evident that the LGHC crystal can be used for opto electronic device fabrication up to the temperature of 185 °C.

3.7. Dielectric studies

The dielectric permittivity and dielectric loss was measured using HIOKI 3532-50 LCR HITESTER model 3532–50 LCR meter. The sample of size 6.78 × 2.75 × 1.82 mm^3 was coated with silver paste to obtain good Ohmic contact. The (011) faceted LGHC crystal was used for the dielectric measurement. The experiment was carried out in the frequency range of 50 Hz to 5 MHz at different temperatures (313, 333, 353 and 373 K). The dielectric permittivity of a crystalline material is a second order tensor. For an orthorhombic system there are three independent components: ε_{11}, ε_{22} and ε_{33} corresponding to *a*, *b* and *c*-directions respectively. The dielectric properties of a crystal may be characterized by the magnitudes and directions of three principal dielectric permittivities [25]. The variation of dielectric permittivity (ε_r), dielectric loss (tan δ) and ac conductivity (σ_{ac}) were measured as a function of frequency at different temperatures.

Dielectric permittivity and Dielectric loss were calculated using the Eqs. (3) and (4)

$$\epsilon_r = \frac{Cd}{\epsilon_0 A} \tag{3}$$

$$\tan\ \delta = \epsilon_r D \tag{4}$$

where *C* is capacitance, *d* is thickness of the sample, $\epsilon_0 = 8.854 \times 10^{-12}$ Fm^{-1} is permittivity of free space, *A* is the area of cross section and *D* is the dissipation factor. Figs. 9 and 10 show the frequency dependency of dielectric permittivity and dielectric loss of LGHC crystal at different temperatures. It was found that the values of dielectric permittivity and dielectric loss decrease with the increase of frequency at all temperatures. As the temperature increases, the value of the dielectric permittivity also increases. The very high values of ε_r and tan δ at low frequencies are due to the presence of all the four polarizations namely, space charge, orientational, ionic and electronic polarizations. As the frequency increases, the space charge cannot sustain and comply with the external field and hence the polarization decreases [26]. According to Miller rule, the low value of dielectric loss at high frequencies revealed the high optical quality of the crystal with less electrically active defects, which is a desirable property for NLO applications [27,28].

Table 3
Comparison of SHG efficiency.

Crystal	Space group	SHG efficiency	Reference
L-Glutamic acid hydrobromide,	$P2_12_12_1$	1.25	[22]
L-Histidine hydrobromide	$P2_12_12_1$	1.6	[23]
L-Arginine hydrochloride monohydrate (LAHCl.H2O)	$P2_1$	0.38	[24]
L-Glutamic acid hydrochloro bromide(LGHCB)	$P2_12_12_1$	1.5	[5]
LGHC	$P2_12_12_1$	0.5	Present work

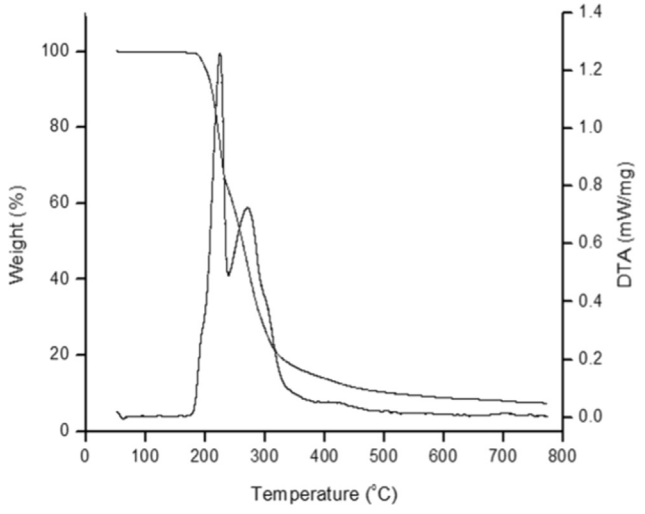

Fig. 8. TGA /DTA thermogram of LGHC.

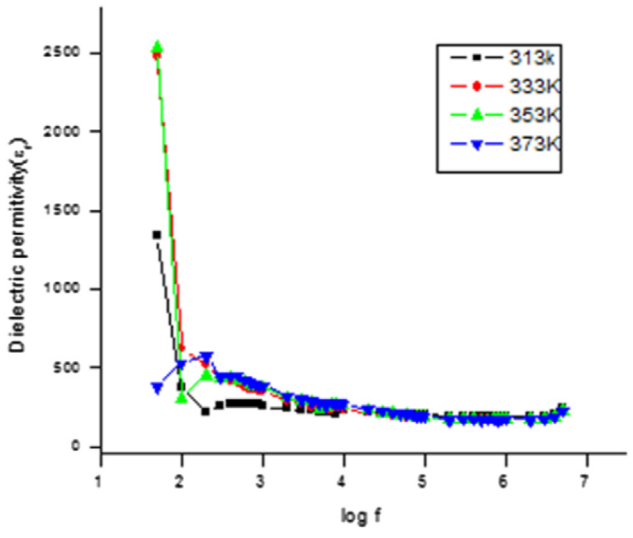

Fig. 9. Dielectric permitivity versus frequency.

The AC conductivity (σ_{ac}) is calculated using the Eq. (5)

$$\sigma_{ac} = \omega\epsilon_0\epsilon_r \tan \delta \quad (5)$$

where $\omega = 2\pi f$, f is the frequency of the applied electric field. The Fig. 11 shows the variation of ac conductivity for different frequencies. It is observed that the ac conductivity feebly increases up to the logarithmic frequency of 6.47 Hz (3 MHz). A sharp increase was observed at the logarithmic frequency of 6.6 Hz (4 MHz) for all the measured temperatures and that indicates the dielectric breakdown frequency of the material.

3.8. Microhardness studies

The mechanical property of the LGHC crystals was studied using SHIMADZU HMV 2 T Vickers hardness tester, fitted with a Vickers's diamond pyramidal indenter. The hardness of the crystal carries information about the strength, molecular bindings, yield strength and elastic constants of the material

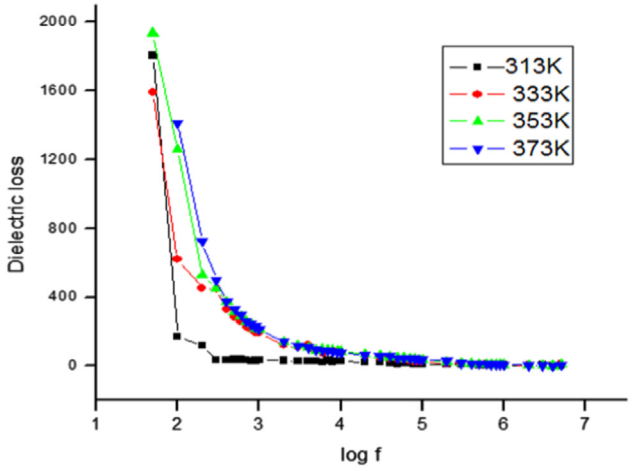

Fig. 10. Dielectric loss versus frequency.

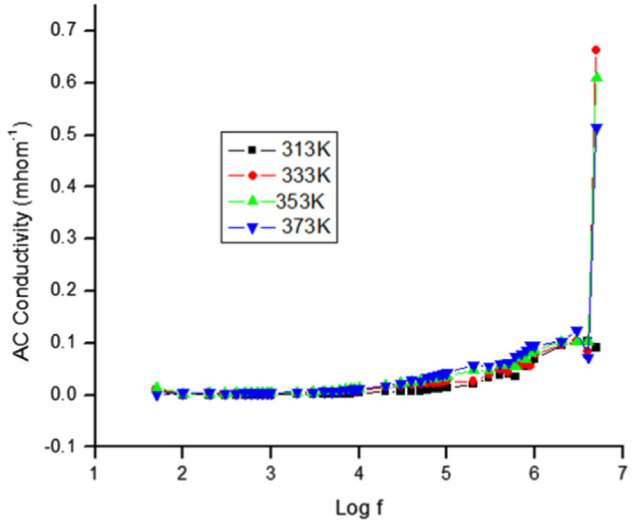

Fig. 11. Log frequency versus ac conductivity.

[29]. The hardness values (H_v) were calculated from Eq. (6)

$$H_v = \frac{1.8544P}{d^2}\text{Kg/mm2} \quad (6)$$

where P is the applied load and d is the mean diagonal length of the indentation. Fig. 12 shows the variation of Vickers's hardness value H_v with the applied load P. It shows that the hardness increases with the increasing load. An increase in the mechanical strength will have significance effect on NLO device fabrication and processing such as ease in polishing and less wastage due to cracking or breakage while polishing [30,31].This can be considered as the reflection of Reverse Indentation Size Effect (RISE) [32,33]. The RISE can be related to energy loss owing to the cracking of the specimen during indentation [34]. Comparison of hardness number for other semiorganic materials for maximum load is shown in Table 4.

Meyer's law [35] relates to load and size of indentation as

$$P = ad^n$$

$$\log P = \log a + n\log d \quad (7)$$

Here, 'a' is the constant for a given material. Using the above Eq. (7) work hardening coefficient/Meyer's index 'n' was determined from the slope of a plot of log d versus log P.

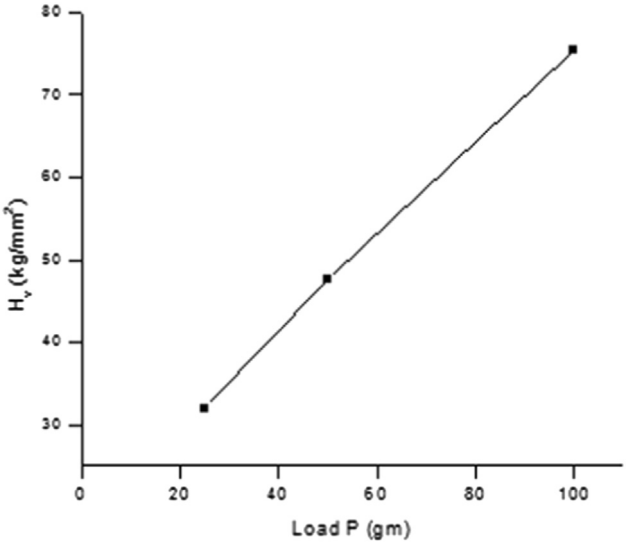

Fig. 12. Vickers hardness number versus load.

Table 4
Comparison of mechanical hardness number for maximum load (100 g).

Crystal	Hardness number (Kg/mm^2)	Reference
LGHC	75.35	Present work
Triglycine zinc chloride (TGZC)	37	[29]
sodium sulfanilate dihydrate (SSDH)	58.2	[25]
Diglycine zinc chloride(DGZC)	107.6	[13]

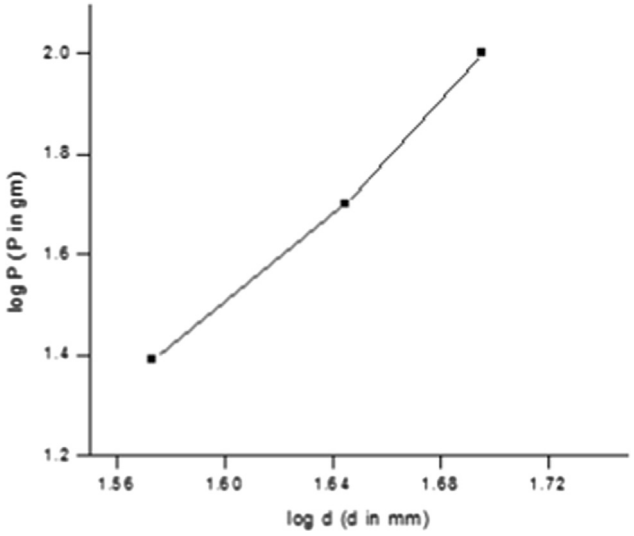

Fig. 13. Plot of log d versus log P.

Table 5
C_{11} and σ_v for various loads.

S.No	Load (gm)	C_{11} ($\times 10^{12}$ Pa)	σ_v ($\times 10^{12}$ Pa)
1	25	14.398	15.020
2	50	27.298	21.648
3	100	61.031	34.284

Fig. 13 shows the plot of log P versus log d fitting data using least-squares fit method and the value of n was found to be 4.94. Vicker hardness increases with the increase of P if $n > 2$ and decreases if $n < 2$. According to Onitsch [36] and Hanneman [37] 'n' should lie between 1 and 1.6 for hard materials and is greater than 1.6 for soft materials. The grown LGHC crystal belongs to soft material category.

The elastic stiffness constant (C_{11}) for different loads is calculated using Wooster's empirical formula [38] $C_{11}=H_v^{7/4}$ shown in Table 2 indicates that the binding forces between the ions are quite strong. For the Meyer's index $n > 2$, Cahoon et al [39] used the formula

$$\sigma_v = \frac{H_v}{2.9}[1-(n-2)]\left[\frac{12.5(n-2)}{[1-(n-2)]}\right]^{(n-2)} \quad (8)$$

for LGHC crystal the yield strength is calculated using the Eq. (8) for various loads and the values are shown in Table 5.

4. Conclusion

Optically good quality single crystal of the L-Glutamic acid Hydrochloride (LGHC) was grown by slow evaporation technique. Single crystal X-Ray Diffraction analysis shows that the crystal belongs to the orthorhombic system with space group $P2_12_12_1$. The Powder X-Ray Diffraction peaks reveal the crystalline nature of the LGHC crystal. The functional groups were confirmed by Fourier Transform Infrared spectral analysis. From UV–vis–NIR studies, a low optical absorption was observed in the entire visible, near infrared region. Lower cut-off wavelength was found to be 248 nm that facilitates the grown crystal to be a potential material for NLO applications. The direct band gap energy for the grown crystal was found to be 5.08 eV. From the refractive index measurements, the index value was found to be 1.4. The SHG efficiency of the grown crystal was found to be 0.5 times more than that of the KDP crystal. Thermal analysis reveals that the sample is thermally stable up to 185 °C. The grown crystal has low value of dielectric permittivity and dielectric loss for higher frequencies at different temperature. The ac conductivity increases with frequency for different temperature. Vickers microhardness reveals that the hardness number H_v increases with increasing load exhibiting Reverse Indentation Size Effect. The value of Meyer's index, 'n' was found to be 4.94 and the grown crystal falls under the soft material category. The values of elastic stiffness constant (C_{11}) and yield strength (σ_v) are calculated. The high value of C_{11} indicates tight bonding between neighboring atoms.

Acknowledgments

The authors thank Sophisticated Analytical Instrument Facility, Indian Institute of Technology, Madras for conducting XRD, UV, FTIR studies and Prof. P. K. Das, Indian Institute of Science, Bangalore for support in SHG measurement. The authors are also thankful to Dr. V.Rajan Babu, VIT University for providing facilities for refractive index studies.

References

[1] D.J. Williams, Angew. Chem. Int. Ed. 23 (1984) 690–703.
[2] N. Vijayan, R. Ramesh Babu, R. Gopalakrishnan, P. Ramasamy, J.Cryst. Growth 267 (2004) 646–653.
[3] M. Fleck, P. Becker, L. Bayarjargal, R. Ochrombel, L. Bohatý, Cryst. Res. Technol. 43 (2008) 127–134.
[4] S. Moitra, T. Kar, Cryst. Res. Technol. 45 (2010) 70–74.
[5] J. Uma, V. Rajendran, J. Therm. Anal. Calorim. 117 (2014) 1157–1163.
[6] R. Sathyalakshmi, V. Kannan, R. Bairava Ganesh, P. Ramasamy, Cryst. Res. Technol. 42 (2007) 78–83.
[7] M. Delfinio, J.P. Dougherty, W.K. Zwicker, M.M. Choy, J. Cryst. Growth 36 (1976) 267–272.
[8] Y.J. Zhang, Z. Shu, W. Xu, G. Chen, Z. Li, Acta Crystallogr. E64 (2008) o446.
[9] M. Delfino, G.M. Loiacono, J.A. Nicolosi, J. Solid State Chem. 23 (1978) 289–296.
[10] K. Selvaraju, R. Valluvan, S. Kumararaman, Mater. Lett. 13 (2006) 1565–1569.
[11] K. Selvaraju, K. Kirubavathi, N. Vijayan, S. Kumararaman, Mod. Phys. Lett. B 23 (2009) 861–870.
[12] R. Bairava Ganesh, V. Kannan, R. Sathyalakshmi, P. Ramasamy, Mater. Lett. 3 (2007) 706–708.
[13] M. Senthil Pandian, P. Ramasamy, J. Cryst. Growth 312 (2010) 413–419.
[14] P. Dhanasekaran, K. Srinivasan, Cryst. Res. Technol. 47 (2012) 1217–1230.
[15] M. Senthil Pandian, K. Boopathi, P. Ramasamy, G. Bhagavannarayana, Mater. Res. Bull. 47 (2012) 826–835.
[16] L.J. Bellamy, in: The Infrared Spectra of Complex Molecules, Wiley, New York, 1995.
[17] M. SenthilPandian, N. Pattanaboonmee, P. Ramasamy, P. Manyum, J. Cryst. Growth 314 (2011) 207–212.

[18] M. Senthil Pandian, P. Ramasamy, Binay Kumar, Mater. Res. Bull. 47 (2012) 1587–1597.
[19] A. Ashour, N. El-Kadry, S.A. Mahmoud, Thin Solid Films 269 (1995) 117–120.
[20] A.K. Chawla, D. Kaur, R. Chandra, Opt. Mater. 29 (2007) 995–998.
[21] K. Kurtz, T.T. Perry, J. Appl. Phys. 39 (1968) 3798–3814.
[22] S. Natarajan, G.P. Chitra, S.A. Martin Britto Dhas, S. Athimoolam, Cryst. Res. Technol. 43 (2008) 713–719.
[23] P. Anandan, G. Parthipan, T. Saravanan, R. MohanKumar, G. Bhagavannarayana, R. Jayavel, Phys. B 405 (2010) 4951–4956.
[24] D. Kalaiselvi, R. Mohan Kumar, R. Jayavel, Cryst. Res. Technol. 43 (2008) 851–856.
[25] M. Senthil Pandian, P. Ramasamy, Mater. Chem. Phys. 132 (2012) 1019–1028.
[26] S.A. Martin Britto Dhas, G. Bhagavannarayana, S. Natarajan, Open Crystallogr. J. 1 (2008) 42–45.
[27] C. Miller, Appl .Phys. Lett. 5 (1964) 17–19.
[28] C. Balarew, R. Duhlew, J. Solid state Chem. 55 (1984) 1–6.
[29] J. Uma, V. Rajendran, Arch. Appl. Sci. Res. 5 (2013) 208–212.
[30] M. Senthil Pandian, N. Balamurugan, V. Ganesh, P.V. Raja Shekar, K. Kishan Rao, P. Ramasamy, Mater. Lett. 62 (2008) 3830–3832.
[31] M. Senthil Pandian, N. Balamurugan, G. Bhagavannarayana, P. Ramasamy, J. Cryst. Growth 310 (2008) 4143–4147.
[32] K. Sangwal, Mater. Chem. Phys. 63 (2000) 145–152.
[33] B. Basu, Mukhopadhyay, N.K. Manisha, J. Eur. Ceram. Soc. 29 (2009) 801–811.
[34] P. Feltham, R. Banerjee, J. Mater. Sci. 27 (1992) 1626–1632.
[35] E. Meyer, Z. Ver. Dtsch. Ing. 52 (1908) 645–654.
[36] E.M. Onitsch, Microskopie 2 (1947) 131–151.
[37] M. Hanneman, Metall. Manchu. 23 (1941) 135–140.
[38] W.A. Wooster, Rep. Prog. Phys. 16 (1953) 62–82.
[39] J.R. Cahoon, W.H. Broughton, A.R. Kutzak, Metall. Trans. 2 (1971) 1979–1983.